

Decentralized and Centralized Optimal Control of HVAC Systems

Thesis Defense

Ryan S. Montrose

April 30, 2021

Boise State University
Department of Mechanical and Biomedical Engineering

Outline

Motivation

Predictive Model

Parameter Estimation

Control Frameworks

Simulation Results

Conclusion

Motivation

U.S. Energy Usage

- ▶ According to the Energy Information Administration, in 2019 the U.S. consumed nearly **100.2** quadrillion Btus (29.4 trillion kWh) of energy.
- ▶ Of this total energy consumption, **11.9** quadrillion Btus (3.5 trillion kWh) were consumed by residential homes.
- ▶ In a residential setting, Thermostatically Controlled Loads (TCLs) constitute the majority of this power consumption.

Major Energy Consuming Devices

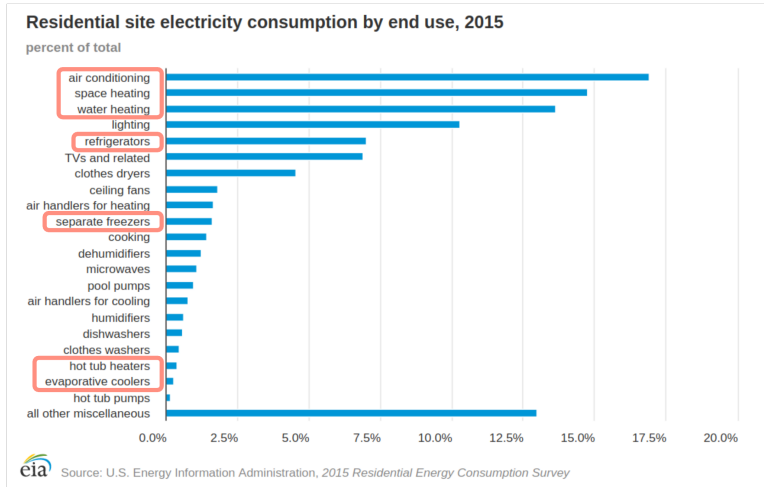


Figure: List of most significant residential energy consuming devices.

Energy Utilities

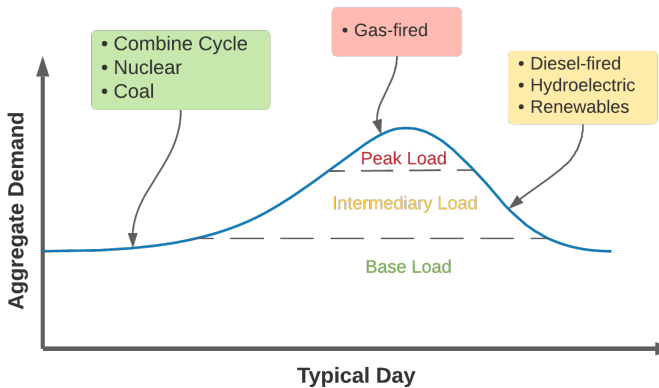


Figure: Summertime aggregate energy consumption profile.

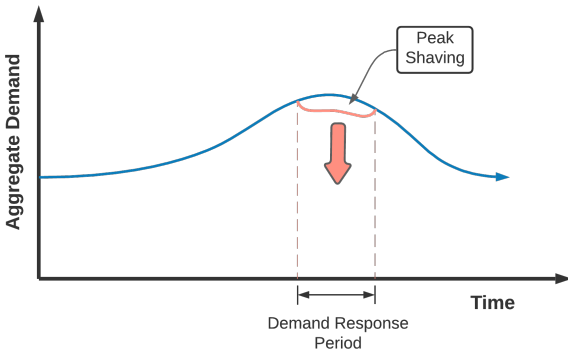
- ▶ Low operation cost, slowly dispatched.
- ▶ High operation cost, quickly dispatched.

Load Types

- ▶ Electric utilities, like Idaho Power, remain competitive by maximizing **base** load production.
- ▶ Accomplished by minimizing costly **intermediary** and **peak** loads.

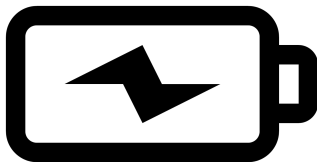
Method of Reducing Peak Demand

- A demand response program is a contractual agreement made between electric utilities and their participating customers to limit energy usage when projected demand threatens the supply of power.



Demand Response Programs – TCLs

- ▶ TCLs are a prime candidate for demand response programs because,
 - ▶ they function like a battery,
 - ▶ exhibit a high degree of flexibility when used,
 - ▶ are readily controlled via the home's smart-meter,
 - ▶ and have the highest potential for power reduction.



Types of Air Conditioning Units

- Single Speed Heat Pumps (SSHP) and Variable Speed Heat Pumps (vSHP) constitute the vast majority of commercially available air conditioning units.

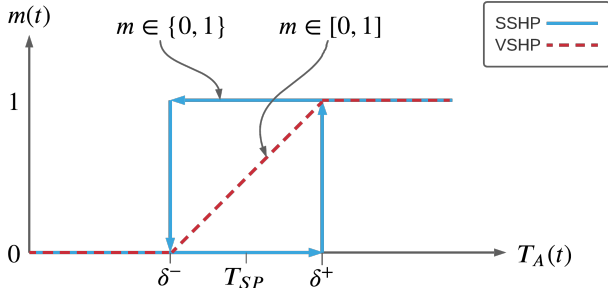


Figure: Single Speed Heat Pump



Figure: Variable Speed Heat Pump 7

Control of SSHP and VSHP Devices



Hysteresis and PID Control

$$m(t) = \begin{cases} 0, & \text{if } T_A \leq \delta^- \\ 1, & \text{if } T_A \geq \delta^+ \\ m(t - \epsilon), & \text{otherwise} \end{cases}$$
$$e(t) = T_{sp} - T_A,$$
$$u(t) = K_P e(t) + K_I \int_0^t e(\tau) d\tau + K_D \frac{d}{dt} e(t),$$
$$m(t) = \text{sat}(u).$$

Baseline Simulation Results

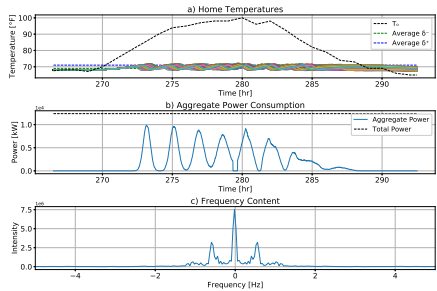


Figure: Hysteresis results ($N=1000$).

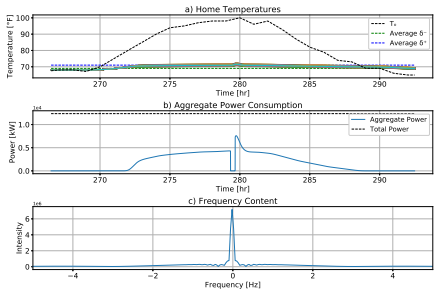


Figure: PID results ($N=1000$).

- Both control frameworks are inherently prone to load synchronization.

Network Communication

- ▶ Past research has focused on network-based coordination to reduce load synchronization [3].

$$A = \begin{bmatrix} 0 & 0 & 0 & 1 & 1 & 0 \\ 0 & 0 & 0 & 1 & 1 & 0 \\ 0 & 0 & 0 & 1 & 0 & 1 \\ 1 & 1 & 1 & 0 & 1 & 1 \\ 1 & 1 & 0 & 1 & 0 & 1 \\ 0 & 0 & 1 & 1 & 1 & 0 \end{bmatrix}$$

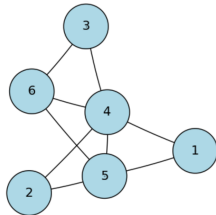


Figure: Adjacency matrix whose elements depict an unweighted and undirected graph.

Population Set : $\mathcal{N} = \{1, \dots, N\}$

Neighbor Set : $\mathcal{N}_p = \{i \in \mathcal{N} \mid a_{p,i} = 1\}$

Connection Degree : $\mathcal{N}_{CD} = \sum_{i \in \mathcal{N}} a_{p,i}$

Advanced Hysteresis Controller – SSHP

$$\begin{aligned}\psi_p^k &= \frac{T_{A,p}^k - \delta_p^-}{\delta_p^+ - \delta_p^-}, \\ \tilde{\mathbf{m}}^k &= \frac{1}{N_{CD}} \mathcal{A} \mathbf{m}^{k-1}.\end{aligned}$$

Hysteresis vs. Advanced Hysteresis

$$m_p^k = \begin{cases} 0, & \text{if } T_{A,p}^k \leq \delta^- \\ 1, & \text{if } T_{A,p}^k \geq \delta^+ \\ m_p^{k-1}, & \text{otherwise} \end{cases} \quad m_p^k = \begin{cases} 0, & \text{if } \psi_p^k \leq K_g \tilde{m}_p^k \\ 1, & \text{if } \psi_p^k \geq K_g \tilde{m}_p^k \\ m_p^{k-1}, & \text{otherwise,} \end{cases}$$

- Advanced hysteresis controller (right) adaptively adjusts dead-band widths to statistically distribute control actions, where K_g is a proportional constant.

SSHP – Advanced Hysteresis Controller Results

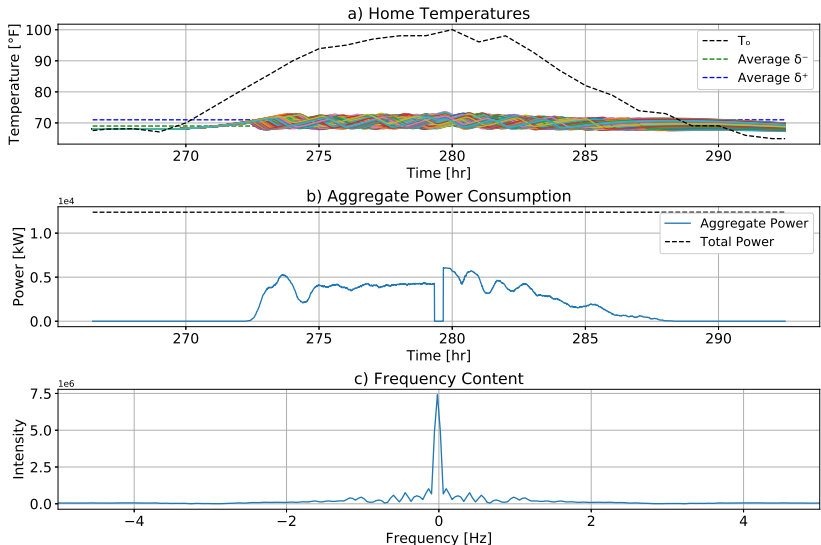


Figure: Simulated Response of advanced hysteresis controller.

Model Predictive Control (MPC)

Model Predictive Control

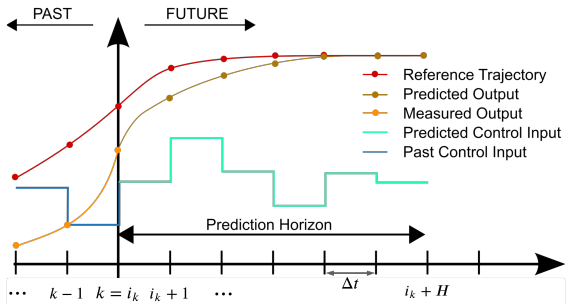


Figure: Model predictive control diagram.

- Generally speaking, an MPC solves for a horizon of control actions, $m^{i_k \in \underline{H}}$, such that the systems' constraints are satisfied and objective is minimized, where $\underline{H} := \{1, \dots, H\}$.

Predictive Model

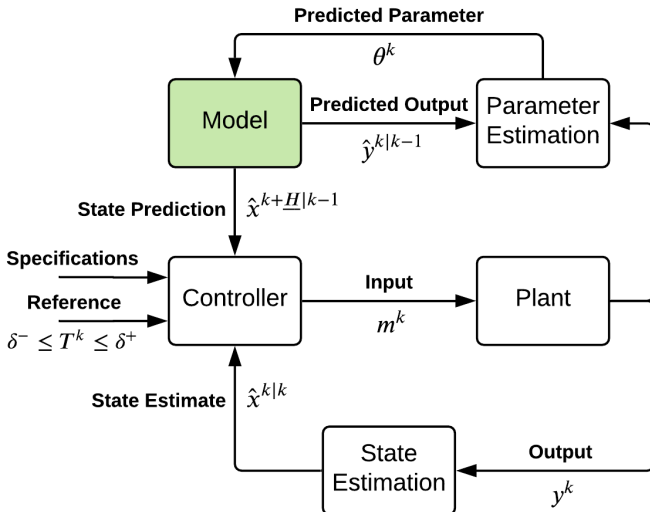


Figure: Model predictive control diagram.

Equivalent Thermal Parameter (ETP) Model

- ▶ A second-order ETP model is used to predict the temperature evolution of a residential home [5].

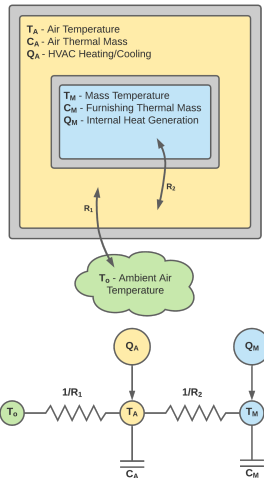


Figure: Thermal circuit diagram.

Predictive Model – Cont.

- ▶ Using the resistive network defined above, two first-order differential equations are formed,

$$C_A \dot{T}_A = Q_A - \frac{1}{R_1} (T_A - T_o) - \frac{1}{R_2} (T_A - T_M), \quad (1)$$

$$C_M \dot{T}_M = Q_M + \frac{1}{R_2} (T_A - T_M). \quad (2)$$

- ▶ When combined, Equations (1) and (2) form a second-order ETP model [2], where $Q_A := \eta m(t)$ (Q_M is neglected),

$$\begin{aligned} & C_M C_A R_2 \ddot{T}_A + \left(C_M \left(\frac{R_2}{R_1} + 1 \right) + C_A \right) \dot{T}_A + \frac{1}{R_1} T_A \\ &= \frac{C_M R_2}{R_1} \dot{T}_o + \frac{1}{R_1} T_o + C_M R_2 \eta \dot{m} + \eta m. \end{aligned} \quad (3)$$

Predictive Model – Cont.

$$\begin{aligned} C_M C_A R_2 \ddot{T}_A + \left(C_M \left(\frac{R_2}{R_1} + 1 \right) + C_A \right) \dot{T}_A + \frac{1}{R_1} T_A \\ = \frac{C_M R_2}{R_1} \dot{T}_o + \frac{1}{R_1} T_o + C_M R_2 \eta \dot{m} + \eta m \end{aligned}$$

- Equation (3) is abbreviated by elements of a parameter vector, $\theta \in \mathbb{R}^5$,

$$\theta_1 \ddot{T}_A + \theta_2 \dot{T}_A + \theta_3 T_A = \theta_4 \dot{T}_o + \theta_5 T_o + \theta_6 \eta \dot{m} + \eta m. \quad (4)$$

- Based on Equation (4), a state space representation is developed for both **SSHP** and **VSHP** devices.

State Space Representation

$$\theta_1 \ddot{T}_A + \theta_2 \dot{T}_A + \theta_3 T_A = \theta_4 \dot{T}_o + \theta_3 T_o + \theta_5 \eta \dot{m} + \eta m.$$

- **SSHP** state space representation ($\theta \in \mathbb{R}^4$, $m \in \{0, 1\}$),

$$\begin{aligned}\dot{x} &= Ax + B \left(\eta m + \theta_4 \dot{T}_o + \theta_3 T_o \right), \\ x^{k+1} &= (I + \Delta t A) x^k + \Delta t B \left(\eta m^k + \theta_4 \dot{T}_o^k + \theta_3 T_o^k \right).\end{aligned}\quad (5)$$

- **VSHP** state space representation (where $\dot{m} = \sigma$, $m \in [0, 1]$),

$$\begin{aligned}\dot{x} &= Ax + B \left(\eta(m + \theta_5 \sigma) + \theta_4 \dot{T}_o + \theta_3 T_o \right), \\ x^{k+1} &= (I + \Delta t A) x^k + \Delta t B \left(\eta \left(m^k + \theta_5 \sigma^k \right) + \theta_4 \dot{T}_o^k + \theta_3 T_o^k \right).\end{aligned}\quad (6)$$

$$x = \begin{bmatrix} T_A \\ \dot{T}_A \end{bmatrix}, \quad A = \begin{bmatrix} 0 & 1 \\ -\frac{\theta_3}{\theta_1} & -\frac{\theta_2}{\theta_1} \end{bmatrix}, \quad B = \begin{bmatrix} 0 \\ \frac{1}{\theta_1} \end{bmatrix}.$$

Parameter Estimation

Parameter Estimation

- ▶ Thermal parameters are expected to have statistical error.
- ▶ Thermal characteristics of a home are expected to change with time:
 - ▶ Building renovation.
 - ▶ Material degradation.

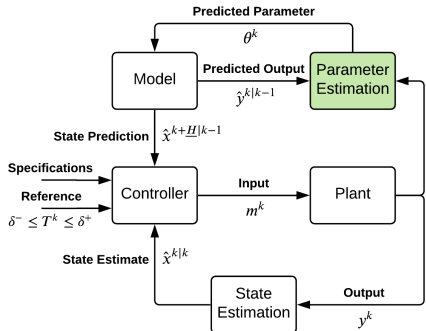


Figure: Parameter estimation via a recursive least squares algorithm.

Recursive Least Squares Algorithm – Cont.

- The RLS algorithm begins by redefining Equation (4) in terms of observer, y_k , and regressor, φ_k , variables.

$$\theta_1 \ddot{T}_A^k + \theta_2 \dot{T}_A^k + \theta_3 T_A^k = \theta_4 \dot{T}_o^k + \theta_3 T_o^k + \eta m^k$$

$$\varphi_k^\top \theta := \theta_1 \ddot{T}_A^k + \theta_2 \dot{T}_A^k + \theta_3 (T_A^k - T_o^k) - \theta_4 \dot{T}_o^k = \eta m^k =: y_k$$

$$\varphi_k^\top = \begin{bmatrix} \ddot{T}_A^k & \dot{T}_A^k & (T_A^k - T_o^k) & -\dot{T}_o^k \end{bmatrix}$$

$$\theta_1 \ddot{T}_A^k + \theta_2 \dot{T}_A^k + \theta_3 T_A^k = \theta_4 \dot{T}_o^k + \theta_3 T_o^k + \theta_5 \eta \dot{m}^k + \eta m^k$$

$$\varphi_k^\top \theta := \theta_1 \ddot{T}_A^k + \theta_2 \dot{T}_A^k + \theta_3 (T_A^k - T_o^k) - \theta_4 \dot{T}_o^k - \theta_5 \eta \dot{m}^k = \eta m^k =: y_k$$

$$\varphi_k^\top = \begin{bmatrix} \ddot{T}_A^k & \dot{T}_A^k & (T_A^k - T_o^k) & -\dot{T}_o^k & -\eta \sigma^k \end{bmatrix}$$

Recursive Least Squares Algorithm – Cont.

- Observer and regressor terms are collected to form the following matrices,

$$Y_{k_s} = \begin{bmatrix} y_1 \\ \vdots \\ y_{k_s} \end{bmatrix}, \quad \Phi_{k_s} = \begin{bmatrix} \varphi_1^\top \\ \vdots \\ \varphi_{k_s}^\top \end{bmatrix}, \quad (7)$$

- where $k_s \in \mathbb{N}$ is chosen such that $\Phi_{k_s}^\top \Phi_{k_s}$ is non-singular.

Recursive Least Squares Algorithm – Cont.

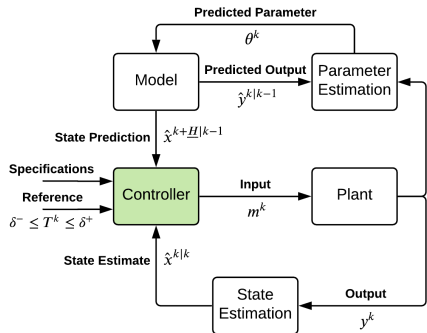
Algorithm 1 RLS with Exponential Forgetting [1]

```
1: Initialize  $P_{k_s} = (\Phi_{k_s}^\top \Phi_{k_s})^{-1}$ 
2: while  $k_s < k \leq K$  do
3:    $S_k = P_{k-1} \varphi_k (\lambda + \varphi_k^\top P_{k-1} \varphi_k)^{-1}$ 
4:    $P_k = (I - S_k \varphi_k^\top) P_{k-1} / \lambda$ 
5:    $\theta_k = \theta_{k-1} + S_k (y_k - \varphi_k^\top \theta_{k-1})$ 
6: end while
```

- ▶ Where $0 < \lambda \in \mathbb{R}$ is the algorithm's exponential forgetting term.
- ▶ Two update conditions are employed,
 - ▶ $\kappa(P_k) \leq c_1$, where $\kappa(\cdot)$ is the condition number, and
 - ▶ $\dot{\theta}_k \leq c_2$.

Centralized and Decentralized Optimal Control

Control of Air Conditioning Systems



- The controller, formulated as an optimization program, solves for a horizon of control actions, $m^{i_k} \in \underline{H}$, subject to the model constraints defined above.

Figure: Optimization based controller

Control Types

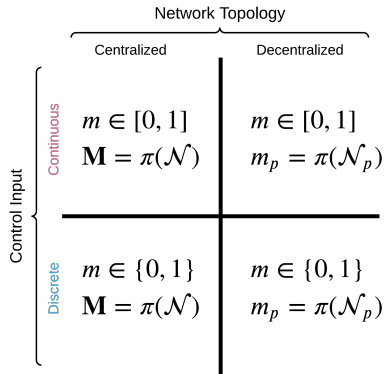


Figure: Optimal control frameworks categorized by input type and network topology.

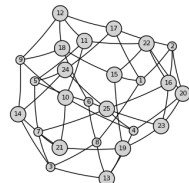


Figure: Decentralized network.

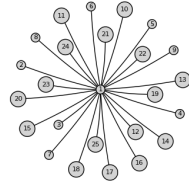


Figure: Centralized network.

Decentralized Discrete (DD) Control – MIQP

$$\begin{aligned} \min_{x, m} \quad & J(k, \mathcal{X}_o) = \sum_{i_k \in \underline{\mathbb{H}}} \ell_{DD}(i_k, x^{i_k}, m^{i_k}) \\ \text{s.t.} \quad & x^1 = \mathcal{X}_o, \\ & x^{i_k+1} = f_{DD}(i_k, x^{i_k}, m^{i_k}, \theta^k), \\ & m^{i_k} \in \{0, 1\}, \\ & \forall i_k \in \underline{\mathbb{H}} := \{1, \dots, H\}, \end{aligned} \tag{8}$$

where

$$f_{DD}(\cdot) = (I + \Delta t A)x^{i_k} + \Delta t B \left(\eta m^{i_k} + \theta_4 \dot{T}_o^{i_k} + \theta_3 T_o^{i_k} \right).$$

DD – Objective

$$\ell_{DD}(\cdot) = -\alpha \left(m^{i_k} - \frac{\sum_{j \in \mathcal{N}_p} m_j^{i_k}}{|\mathcal{N}_p|} \right)^2 - \beta \eta m^{i_k} + \gamma \tilde{T}^{i_k} + \zeta (\dot{T}_A^{i_k})^2$$

- ▶ $-\alpha \left(m^{i_k} - \frac{\sum_{j \in \mathcal{N}_p} m_j^{i_k}}{|\mathcal{N}_p|} \right)^2$ maximizes the difference in control action between the p^{th} agent and its neighbor-set \mathcal{N}_p .
- ▶ $-\beta \eta m^{i_k}$ minimizes individual power consumption.
- ▶ $\gamma \tilde{T}^{i_k}$ minimizes indoor temperature deviations from the dead-band, where $\tilde{T}^{i_k} := \max \left(\delta^- - T_A^{i_k}, 0, T_A^{i_k} - \delta^+ \right)$.
- ▶ $\zeta (\dot{T}_A^{i_k})^2$ minimizes the indoor air temperature's rate of change.

Temperature Soft Constraint

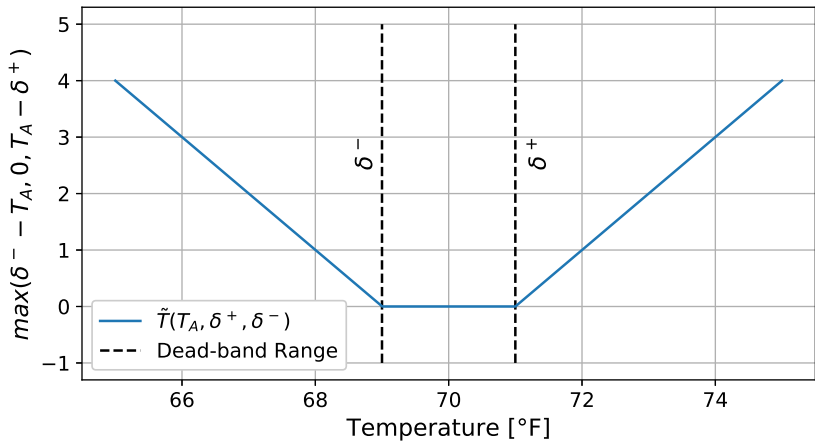


Figure: Double-hinge soft constraint penalizes temperature excursions.

Tuning

$$\ell_{DD}(\cdot) = -\alpha \left(m^{i_k} - \frac{\sum_{j \in \mathcal{N}_p} m_j^{i_k}}{|\mathcal{N}_p|} \right)^2 - \beta \eta m^{i_k} + \gamma \tilde{T}^{i_k} + \zeta (\dot{T}_A^{i_k})^2$$

- ▶ α, β, γ , and ζ , much like knobs on a dial, tune the desired response of the optimization program.
- ▶ The relative magnitudes determine the controller's response.
- ▶ Objective constants are chosen such that aggregate temperature and power requirements are balanced.

Centralized Discrete (CD) Control – MIQP

$$\begin{aligned}
 \min_{X, M} \quad & J(k, \mathcal{X}_o) = \sum_{i_k \in \underline{\mathbb{H}}} \left(g_{CD}(i_k, M^{i_k}) + \ell_{CD}(i_k, X^{i_k}, M^{i_k}) \right) \\
 \text{s.t.} \quad & x_p^1 = \mathcal{X}_{o,p}, \\
 & x_p^{i_k+1} = f_{CD}(p, i_k, x_p^{i_k}, m_p^{i_k}, \theta_p^k), \\
 & m_p^{i_k} \in \{0, 1\}, \\
 & \forall p \in \mathcal{N}, \forall i_k \in \underline{\mathbb{H}},
 \end{aligned} \tag{9}$$

where $X^{i_k} = [x_1^{i_k}]^\top, \dots, [x_N^{i_k}]^\top]^\top$, $M^{i_k} = [m_1^{i_k}, \dots, m_N^{i_k}]^\top$, and

$$f_{CD}(p, \cdot) = (I + \Delta t A)x_p^{i_k} + \Delta t B \left(\eta m_p^{i_k} + \theta_4 \dot{T}_o^{i_k} + \theta_3 T_o^{i_k} \right).$$

CD – Objective

$$g_{CD}(\cdot) = \alpha \sum_{z=0}^{z_m} \left(\xi^{(z)} \left| \sum_{p \in \mathcal{N}} m_p^{i_k-z} - m_p^{i_k-z-1} \right| \right),$$

$$\ell_{CD}(\cdot) = \sum_{p \in \mathcal{N}} -\beta \eta m_p^{i_k} + \gamma \tilde{T}_p^{i_k} + \zeta (\dot{T}_{A,p}^{i_k})^2.$$

- ▶ $\alpha \sum_{z=0}^{z_m} \left(\xi^{(z)} \left| \sum_{p \in \mathcal{N}} m_p^{i_k-z} - m_p^{i_k-z-1} \right| \right)$ minimizes the difference in aggregate control actions along a decremented sliding window.

Decentralized Continuous (DC) Control – QP

$$\begin{aligned} \min_{x, m, \sigma} \quad & J(k, \mathcal{X}_o) = \sum_{i_k \in \underline{\mathbb{H}}} \ell_{DC} \left(i_k, x^{i_k}, m^{i_k}, \sigma^{i_k} \right) \\ \text{s.t.} \quad & x^1 = \mathcal{X}_o, \\ & m^{i_k} \in [0, 1], \\ & m^{i_k+1} = m^{i_k} + \Delta t \sigma^{i_k}, \\ & x^{i_k+1} = f_{DC} \left(i_k, x^{i_k}, m^{i_k}, \sigma^{i_k}, \theta^k \right), \\ & \forall i_k \in \underline{\mathbb{H}}, \end{aligned} \tag{10}$$

where

$$f_{DC}(\cdot) = (I + \Delta t A)x^{i_k} + \Delta t B \left(\eta \left(m^{i_k} + \theta_5 \sigma^{i_k} \right) + \theta_4 \dot{T}_o^{i_k} + \theta_3 T_o^{i_k} \right).$$

DC – Objective

$$\ell_{DC}(\cdot) = \alpha \left(m^{i_k} - \frac{\sum_{j \in \mathcal{N}_p} m_j^{i_k}}{|\mathcal{N}_p|} \right)^2 - \beta \eta m^{i_k} + \gamma \tilde{T}^{i_k} \\ + \zeta (\dot{T}_A^{i_k})^2 + \tau (\sigma^{i_k})^2$$

- ▶ $\alpha \left(m^{i_k} - \frac{\sum_{j \in \mathcal{N}_p} m_j^{i_k}}{|\mathcal{N}_p|} \right)^2$ now **minimizes** the difference in control action between the p^{th} agent and it's neighbor-set \mathcal{N}_p .
- ▶ $\tau (\sigma^{i_k})^2$ minimizes the rate which $m^{i_k} \in [0, 1]$ changes.

Centralized Continuous (CC) Control – QP

$$\begin{aligned}
 \min_{X, M, \sigma} \quad & J(k, \mathcal{X}_o) = \sum_{i_k \in \underline{\mathbb{H}}} \ell_{CC} \left(i_k, X^{i_k}, M^{i_k}, \sigma^{i_k} \right) \\
 \text{s.t.} \quad & x_p^1 = \mathcal{X}_{o,p}, \\
 & m_p^{i_k} \in [0, 1], \\
 & m_p^{i_k+1} = m_p^{i_k} + \Delta t \sigma_p^{i_k}, \\
 & x_p^{i_k+1} = f_{CC} \left(p, i_k, x_p^{i_k}, m_p^{i_k}, \sigma_p^{i_k}, \theta_p^k \right), \\
 & \forall p \in \mathcal{N}, \forall i_k \in \underline{\mathbb{H}},
 \end{aligned} \tag{11}$$

where $X^{i_k} = [x_1^{i_k}^\top, \dots, x_N^{i_k}^\top]^\top$, $M^{i_k} = [m_1^{i_k}, \dots, m_N^{i_k}]^\top$, and

$$f_{CC}(p, \cdot) = (I + \Delta t A) x_p^{i_k} + \Delta t B \left(\eta \left(m_p^{i_k} + \theta_5 \sigma_p^{i_k} \right) + \theta_4 \dot{T}_o^{i_k} + \theta_3 T_o^{i_k} \right).$$

CC – Objective

$$\ell_{CC}(\cdot) = \alpha \left| \sum_{p \in \mathcal{N}} m_p^{i_k+1} + m_p^{i_k} \right| + \sum_{p \in \mathcal{N}} -\beta \eta_p m_p^{i_k} + \gamma \tilde{T}_p^{i_k} + \zeta (\dot{T}_{A,p}^{i_k})^2 + \tau (\sigma_p^{i_k})^2.$$

- $\alpha \left| \sum_{p \in \mathcal{N}} m_p^{i_k+1} + m_p^{i_k} \right|$ minimizes the difference in aggregate control effort between adjacent time-steps.

Simulation Results

Thermal Parameter Values

Table: Thermal Parameters.

Thermal Parameter	Mean	Std.
$C_A \left[\frac{Btu}{^{\circ}F} \right]$	1,080	54
$C_M \left[\frac{Btu}{^{\circ}F} \right]$	4,280	214
$\frac{1}{R_1} \left[\frac{Btu}{^{\circ}F \cdot hr} \right]$	520	26
$\frac{1}{R_2} \left[\frac{Btu}{^{\circ}F \cdot hr} \right]$	7,050	353

Other Parameter Values

Table: Simulation parameters

	(H)	(AH)	(PID)	(DD)	(CD)	(DC)	(cc)				
α	-	-	-	300	1,000	200	300				
β	-	-	-	0.001	0.001	0.001	0.001				
γ	-	-	-	5,000	1,200	5,000	8,000				
ζ	-	-	-	0.01	-	100	100				
τ	-	-	-	-	-	1,000	1,500				
Homes (N)	1,000			50							
Time-step (K)	4,000										
Horizon (H)	-	-	-	20							
Step-length (Δt)	23.4 [sec]										
D.R. period	20 [min]										

Decentralized MPC Algorithm

Algorithm 2 Decentralized MPC Sequence

```
Initialize  $\mathcal{P} \leftarrow \emptyset, \mathcal{D} \leftarrow \emptyset$ 
 $\mathcal{P} \leftarrow \text{Generate } \theta_0$ 
 $\mathcal{D} \leftarrow \text{Set Initial Conditions}$ 
for  $k = 1$  to  $K$  do
    for  $p = 1$  to  $N$  do
         $m_p^{i_k \in \mathbb{H}} \leftarrow \text{Controller}(\mathcal{D}, \mathcal{P}, k, p)$ 
         $x_p^k \leftarrow \text{Plant}(\mathcal{D}, \mathcal{P}, k, p, m_p^k)$ 
         $\mathcal{D} \leftarrow x_p^k, m_p^{i_k \in \mathbb{H}}$ 
    end for
    if  $k \geq 2$  then
         $\mathcal{D} \leftarrow \text{Lockout}(\mathcal{D})$ 
         $\mathcal{P} \leftarrow \text{Algorithm (1)}$ 
    end if
end for
```

Centralized MPC Algorithm

Algorithm 3 Centralized MPC Sequence

```
Initialize  $\mathcal{P} \leftarrow \emptyset, \mathcal{D} \leftarrow \emptyset$ 
 $\mathcal{P} \leftarrow \text{Generate } \theta_0$ 
 $\mathcal{D} \leftarrow \text{Set Initial Conditions}$ 
for  $k = 1$  to  $K$  do
     $M^{i_k \in \underline{H}} \leftarrow \text{Controller}(\mathcal{D}, \mathcal{P}, k)$ 
     $X^k \leftarrow \text{Plant}(\mathcal{D}, \mathcal{P}, k, M^k)$ 
     $\mathcal{D} \leftarrow X^k, M^{i_k \in \underline{H}}$ 
    if  $k \geq 2$  then
         $\mathcal{D} \leftarrow \text{Lockout}(\mathcal{D})$ 
         $\mathcal{P} \leftarrow \text{Algorithm (1)}$ 
    end if
end for
```

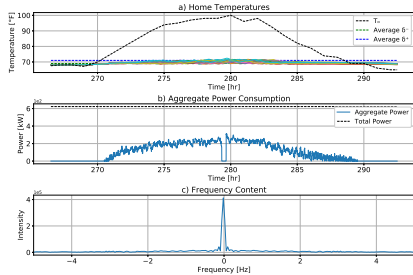


Figure: DD results ($N=50$).

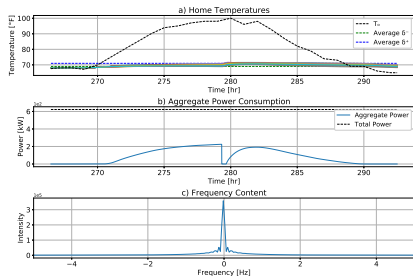


Figure: DC results ($N=50$).

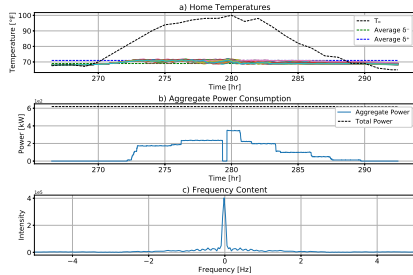


Figure: CD results ($N=50$).

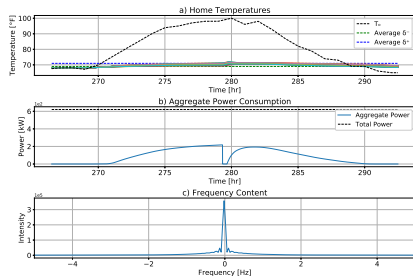
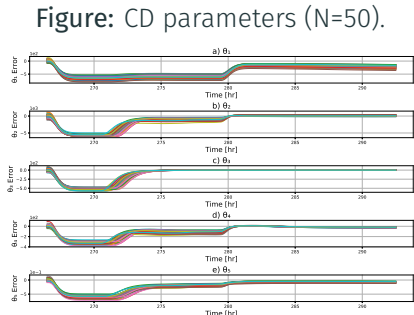
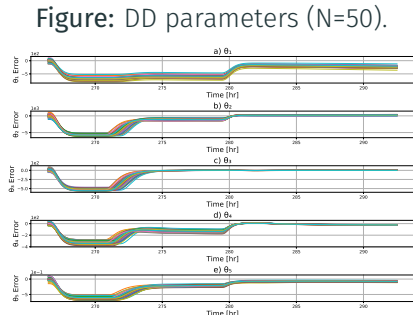
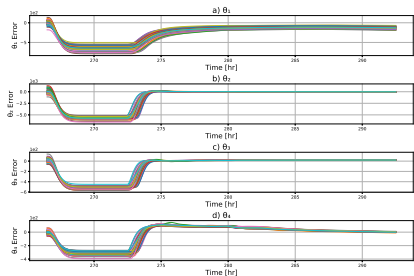
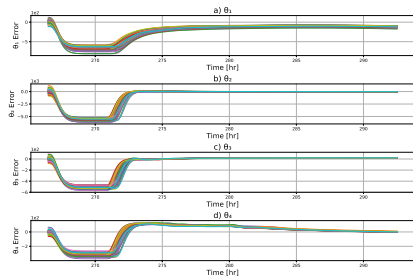


Figure: CC results ($N=50$).



Comparison

- ▶ t_{dev} – Total time a population spends above its upper dead-band threshold δ^+ .
- ▶ P_i, P_f – Ratios between the total consumable power and the maximum power consumed before and after the demand response event.
- ▶ E_T – Ratio between the total available energy in the system and the energy expended during operation.

Controller Type	t_{dev} [hrs/TCL]	P_i	P_f	E_T
Hysteresis	0.81	79.7%	73.6%	15.2%
Advanced Hysteresis	3.05	42.5%	49.0%	15.0%
PID	0.80	35.9%	61.4%	14.5%
Decentralized Discrete	0.36	44.1%	50.0%	16.6%
Centralized Discrete	3.04	38.4%	56.5%	16.3%
Decentralized Continuous	0.72	36.1%	30.8%	14.4%
Centralized Continuous	1.02	35.1%	31.1%	14.4%

Key Observations

- ▶ Load synchronization is significantly reduced with peer-to-peer coordination.
- ▶ Little difference is observed between centralized and decentralized network topologies.
 - ▶ Important because it suggests with limited communication our decentralized frameworks get near omniscient results.
- ▶ Centralized control frameworks are burdened with a combinatorial computational complexity.
- ▶ Parameter estimation indeed converges upon the ‘actual’ plant dynamics.

Key Observations – Cont.

- ▶ Both continuous control frameworks benefit from minimizing the control input's rate of change.
 - ▶ Allows gradual changes in aggregate power consumption.
- ▶ No distinguishable difference is observed between continuous control frameworks.
- ▶ Unlike the advance hysteresis framework, temperature need not be sacrificed for marginal aggregate power stability.
- ▶ Continuous control frameworks struggle with estimating thermal parameters.
 - ▶ Attributed to the lack of persistence of excitation.

Conclusion

Conclusion

- ▶ The main contribution of this research is the development of decentralized control frameworks which regulate **SSH**P and **VSH**P devices.
- ▶ We build upon the well established second-order ETP model by employing a RLS algorithm.
- ▶ We introduce a novel approach by considering $\sigma := \dot{m}$ as the **VSH**P control input.

Bibliography i

- [1] Karl J Åström and Björn Wittenmark. Adaptive control. Courier Corporation, 2013.
- [2] Jason Fuller. Residential module user's guide, 2017. URL http://gridlab-d.shoutwiki.com/wiki/Residential_module_user's_guide.
- [3] Jason Kuwada, Ryan Schwartz, and John F Gardner. Local communication in populations of thermostatically controlled loads. ASME Journal of Engineering for Sustainable Buildings and Cities, 1(3), 2020.

Bibliography ii

- [4] Eerotokritos Xydas, Charalampos Marmaras, and Liana M Cipcigan. A multi-agent based scheduling algorithm for adaptive electric vehicles charging. Applied energy, 177: 354–365, 2016.
- [5] Wei Zhang, Jianming Lian, Chin-Yao Chang, and Karanjit Kalsi. Aggregated modeling and control of air conditioning loads for demand response. IEEE transactions on power systems, 28(4):4655–4664, 2013.

Appendix – Second Order ETP Derivation

$$C_A \dot{T}_A = Q_A - \frac{1}{R_1} (T_A - T_o) - \frac{1}{R_2} (T_A - T_M), \quad (12)$$

$$C_M \dot{T}_M = Q_M + \frac{1}{R_2} (T_A - T_M). \quad (13)$$

A second-order equivalent thermal parameter model is created from Figure 11 by first rewriting Equation (12) in terms of T_M ,

$$T_M = R_2 C_A \dot{T}_A + \left(\frac{R_2}{R_1} + 1 \right) T_A - R_2 Q_A - \frac{R_2}{R_1} T_o. \quad (14)$$

Next, take the derivative of Equation (14) with respect to time,

$$\dot{T}_M = R_2 C_A \ddot{T}_A + \left(\frac{R_2}{R_1} + 1 \right) \dot{T}_A - R_2 \dot{Q}_A - \frac{R_2}{R_1} \dot{T}_o. \quad (15)$$

Appendix – Second Order ETP Derivation Cont.

Substitute Equations (14) and (15) into Equation (13) then simplify,

$$\begin{aligned} C_A C_M R_2 \ddot{T}_A + \left(C_M \left(\frac{R_2}{R_1} + 1 \right) + C_A \right) + \frac{1}{R_1} T_A = \\ Q_M + Q_A + C_M R_2 \dot{Q}_A + \frac{1}{R_1} T_o + C_M \frac{R_2}{R_1} \dot{T}_o \end{aligned}$$

This concludes the derivation of the second-order ETP model.

Appendix – Signal Conditioning

- Once calculated, newly estimated parameters are passed through a low-pass filter to reduce measurement noise,

$$\theta_k = a_0 \theta_k + \sum_{i=1}^4 b_i \theta_{k-i}, \quad (16)$$

where

$$\begin{bmatrix} a_0 \\ b_1 \\ b_2 \\ b_3 \\ b_4 \end{bmatrix} = \begin{bmatrix} (1-z)^4 \\ 4z \\ -6z^2 \\ 4z^3 \\ -z^4 \end{bmatrix},$$
$$z = e^{-14.445f_c}.$$

$$f_c = \frac{\Delta t}{3}.$$

Grid-Level Battery Storage and Solar Panels

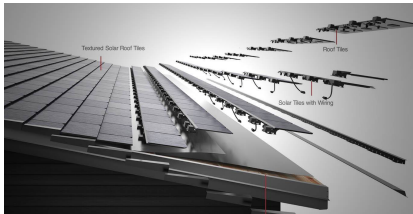


Figure: Solar Roof¹



Figure: Power Wall¹

- ▶ This solution is costly, therefore, inaccessible to the general public [4].
- ▶ Contributes to the ever-increasing Duck Curve.

¹Courtesy of Tesla Motor Company

Duck Curve

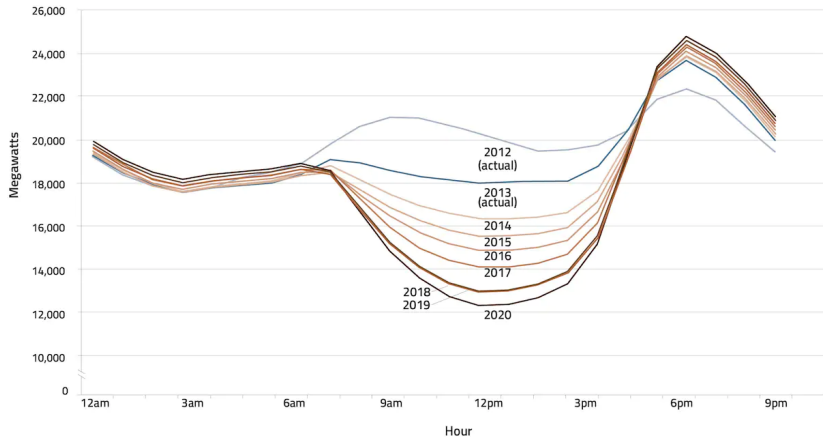


Figure: Duck curve showing increased levels of midday renewable energy saturation²

²Duck Curve, courtesy of the California Independent Systems Operator.

Appendix – Decentralized Discrete Results

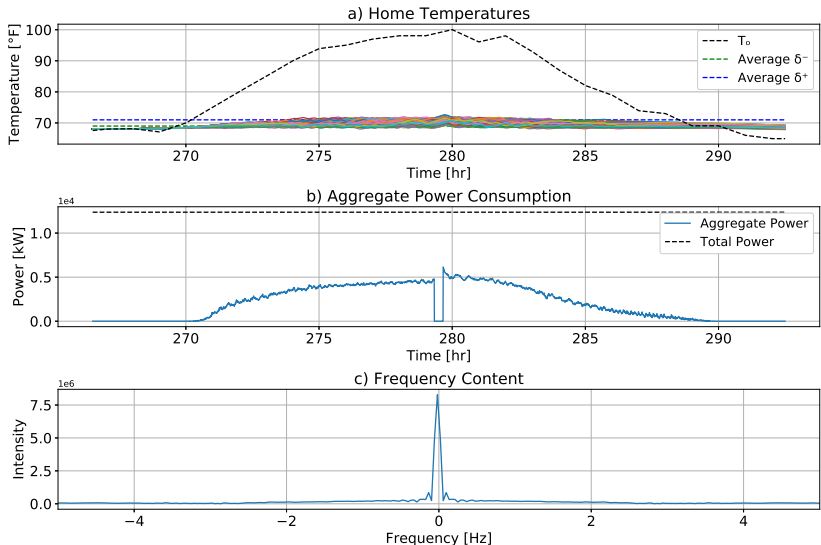


Figure: DD results ($N = 1,000$).

Appendix – Closed Loop Diagram

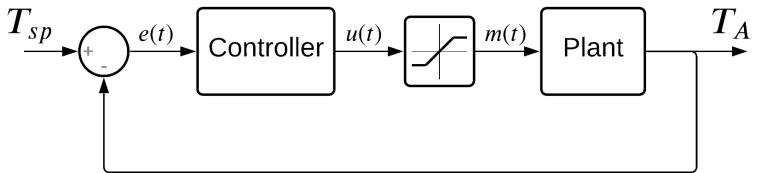


Figure: PID closed loop control diagram.